LETTER

doi:10.1038/nature09746

The structural basis for agonist and partial agonist action on a β_1–adrenergic receptor

Tony Warne[1], Rouslan Moukhametzianov[1], Jillian G. Baker[2], Rony Nehmé[1], Patricia C. Edwards[1], Andrew G. W. Leslie[1], Gebhard F. X. Schertler[1]† & Christopher G. Tate[1]

β-adrenergic receptors (βARs) are G-protein-coupled receptors (GPCRs) that activate intracellular G proteins upon binding catecholamine agonist ligands such as adrenaline and noradrenaline[1,2]. Synthetic ligands have been developed that either activate or inhibit βARs for the treatment of asthma, hypertension or cardiac dysfunction. These ligands are classified as either full agonists, partial agonists or antagonists, depending on whether the cellular response is similar to that of the native ligand, reduced or inhibited, respectively. However, the structural basis for these different ligand efficacies is unknown. Here we present four crystal structures of the thermostabilized turkey (*Meleagris gallopavo*) β_1-adrenergic receptor (β_1AR-m23) bound to the full agonists carmoterol and isoprenaline and the partial agonists salbutamol and dobutamine. In each case, agonist binding induces a 1 Å contraction of the catecholamine-binding pocket relative to the antagonist bound receptor. Full agonists can form hydrogen bonds with two conserved serine residues in transmembrane helix 5 ($Ser^{5.42}$ and $Ser^{5.46}$), but partial agonists only interact with $Ser^{5.42}$ (superscripts refer to Ballesteros–Weinstein numbering[3]). The structures provide an understanding of the pharmacological differences between different ligand classes, illuminating how GPCRs function and providing a solid foundation for the structure-based design of novel ligands with predictable efficacies.

Determining how agonists and antagonists bind to the β receptors has been the goal of research for more than 20 years[4–11]. Although the structures of the homologous β_1 and β_2 receptors[12–15] show how some antagonists bind to receptors in the inactive state[16], structures with agonists bound are required to understand subsequent structural transitions involved in activation. GPCRs exist in an equilibrium between an inactive state (R) and an activated state (R*) that can couple and activate G proteins[17]. The binding of a full agonist, such as adrenaline or noradrenaline, is thought to increase the probability of the receptor converting to R*, with a conformation similar to that of opsin[18,19]. In the absence of any ligand, the βARs exhibit a low level of constitutive activity, indicating that there is always a small proportion of the receptor in the activated state, with the β_2AR showing a fivefold higher level of basal activity than the β_1AR[20]. Basal activity of β_2AR is important physiologically, as shown by the $T164I^{4.56}$ human polymorphism that reduces the basal activity of β_2AR to levels similar to β_1AR[21] and whose expression has been associated with heart disease[22].

As a first step towards understanding how agonists activate receptors, we have determined the structures of β_1AR bound to four different agonists. Native turkey β_1AR is unstable in detergent[23], so crystallization and structure determination relied on using a thermostabilized construct (β_1AR-m23) that contained six point mutations, which dramatically improved its thermostability[24]. In addition, the thermostabilizing mutations altered the equilibrium between R and R*, so that the receptor was preferentially in the R state[24]. However, it could still couple to G proteins after activation by agonists[13] (Supplementary Fig. 1 and Supplementary Tables 1–3), although the activation energy barrier is predicted to be considerably higher than for the wild-type receptor[25]. Here we report structures of β_1AR-m23 (see Methods) bound to R-isoprenaline (2.85 Å resolution), R,R-carmoterol (2.6 Å resolution), R-salbutamol (3.05 Å resolution) and R-dobutamine (two independent structures at 2.6 Å and 2.5 Å resolution) (Supplementary Table 5). The overall structures of β_1AR-m23 bound to the agonists are very similar to the structure with the bound antagonist cyanopindolol[13], as expected for a receptor mutant stabilized preferentially in the R state. None of the structures show the outward movement of the cytoplasmic end of transmembrane helix H6 by 5–6 Å that is observed during light activation of rhodopsin[18,19,26]. This indicates that the structures represent an inactive, non-signalling state of the receptor formed on initial agonist binding.

All four agonists bind in the catecholamine pocket in a virtually identical fashion (Fig. 1). The secondary amine and β-hydroxyl groups shared by all the agonists (except for dobutamine, which lacks the β-hydroxyl; see Supplementary Fig. 4) form potential hydrogen bonds with $Asp\,121^{3.32}$ and $Asn\,329^{7.39}$, whereas the hydrogen bond donor/acceptor group equivalent to the catecholamine *meta*-hydroxyl (*m*-OH) generally forms a hydrogen bond with $Asn\,310^{6.55}$. In addition, all the agonists can form a hydrogen bond with $Ser\,211^{5.42}$, as seen for cyanopindolol[13], and they also induce the rotamer conformation change of $Ser\,212^{5.43}$ so that it makes a hydrogen bond with $Asn\,310^{6.55}$. The major difference between the binding of full agonists compared to the partial agonists is that only full agonists make a hydrogen bond to the side chain of $Ser\,215^{5.46}$ as a result of a change in side chain rotamer. All of these amino acid residues involved in the binding of the catecholamine headgroups to β_1AR are fully conserved in both β_1 and β_2 receptors (Fig. 2). Furthermore, the role of many of these amino acid residues in ligand binding is supported by extensive mutagenesis studies on β_2AR that were performed before the first β_2AR structure was determined[27]. Thus it was predicted that $Asp\,113^{3.32}$, $Ser\,203^{5.42}$, $Ser\,207^{5.46}$, $Asn\,293^{6.55}$ and $Asn\,312^{7.39}$ in β_2AR were all involved in agonist binding[4,5,7–9] (Fig. 3). Inspection of the region outside the catecholamine binding pocket in the structures with bound dobutamine and carmoterol allows the identification of non-conserved residues that interact with these ligands (Fig. 2 and Supplementary Fig. 7), which may contribute to the subtype specificity of these ligands[10,28].

There are three significant differences in the β_1AR catecholamine binding pocket when full agonists are bound compared to when an antagonist is bound, namely the rotamer conformation changes of side chains $Ser\,212^{5.43}$ and $Ser\,215^{5.46}$ (Fig. 3) and the contraction of the catecholamine binding pocket by ~1 Å, as measured between the Cα atoms of $Asn\,329^{7.39}$ and $Ser\,211^{5.42}$ (Fig. 4). So why should these small changes increase the probability of R* formation? Agonist binding has not changed the conformation of transmembrane helix H5 below $Ser\,215^{5.46}$, although significant changes in this region are predicted once the receptor has reached the fully activated state[18,19]. The only effect that the agonist-induced rotamer conformation change of $Ser\,215^{5.46}$ appears to have is to break the van der Waals interaction between $Val\,172^{4.56}$ and $Ser\,215^{5.46}$, thus reducing the number of interactions

[1]MRC Laboratory of Molecular Biology, Hills Road, Cambridge CB2 0QH, UK. [2]Institute of Cell Signalling, C Floor Medical School, Queen's Medical Centre, University of Nottingham, Nottingham NG7 2UH, UK. †Present address: Paul Scherrer Institut, Laboratory of Biomolecular Research, BMR, OFLC 109, CH-5232 Villigen PSI, Switzerland.

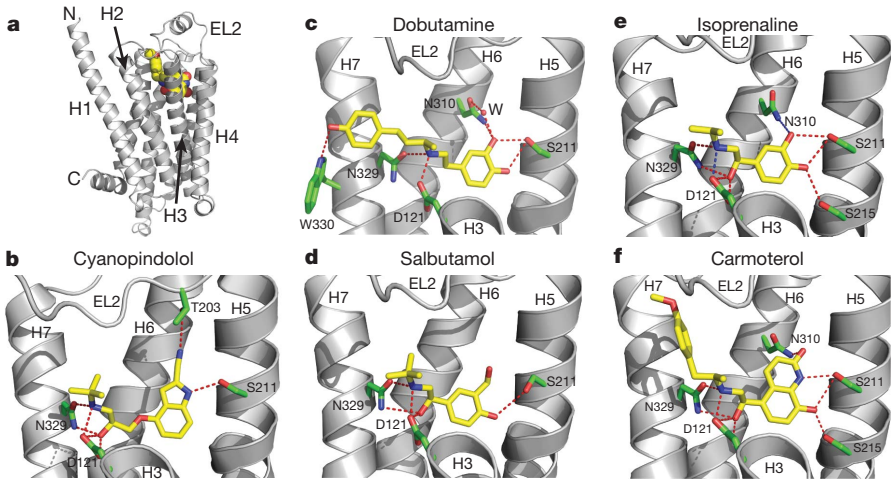

Figure 1 | Structure of the β_1-adrenergic receptor bound to agonists. **a**, Structure of β_1AR shown in cartoon representation with the intracellular side at the bottom of the figure. The ligand carmoterol is shown as a space filling model (C, yellow; O, red; N, blue). The amino terminus (N), carboxy terminus (C), extracellular loop 2 (EL2), and transmembrane helices 1–4 (H1–H4) are labelled. **b**–**f**, The same orientation of receptor is shown in panels **b**, the antagonist cyanopindolol; **c**, **d**, the partial agonists dobutamine and salbutamol; **e**, **f**, the full agonists isoprenaline and carmoterol. The colour scheme of the ligand and labelling of the receptor is identical in all panels, with amino acid side chains that make hydrogen bonds to the ligands depicted (C, green; O, red; N, blue). For clarity, residues 171–196 and 94–119 have been removed in **b**–**f**, which correspond to the C-terminal region of H4 and EL2, and EL1 with the C-terminal region of H2 and N-terminal region of H3, respectively. All structures shown are of monomer B (Supplementary Fig. 2) and were generated using Pymol (DeLano Scientific). For a comparison of the positions of the ligands when bound to the receptor, see Supplementary Fig. 5.

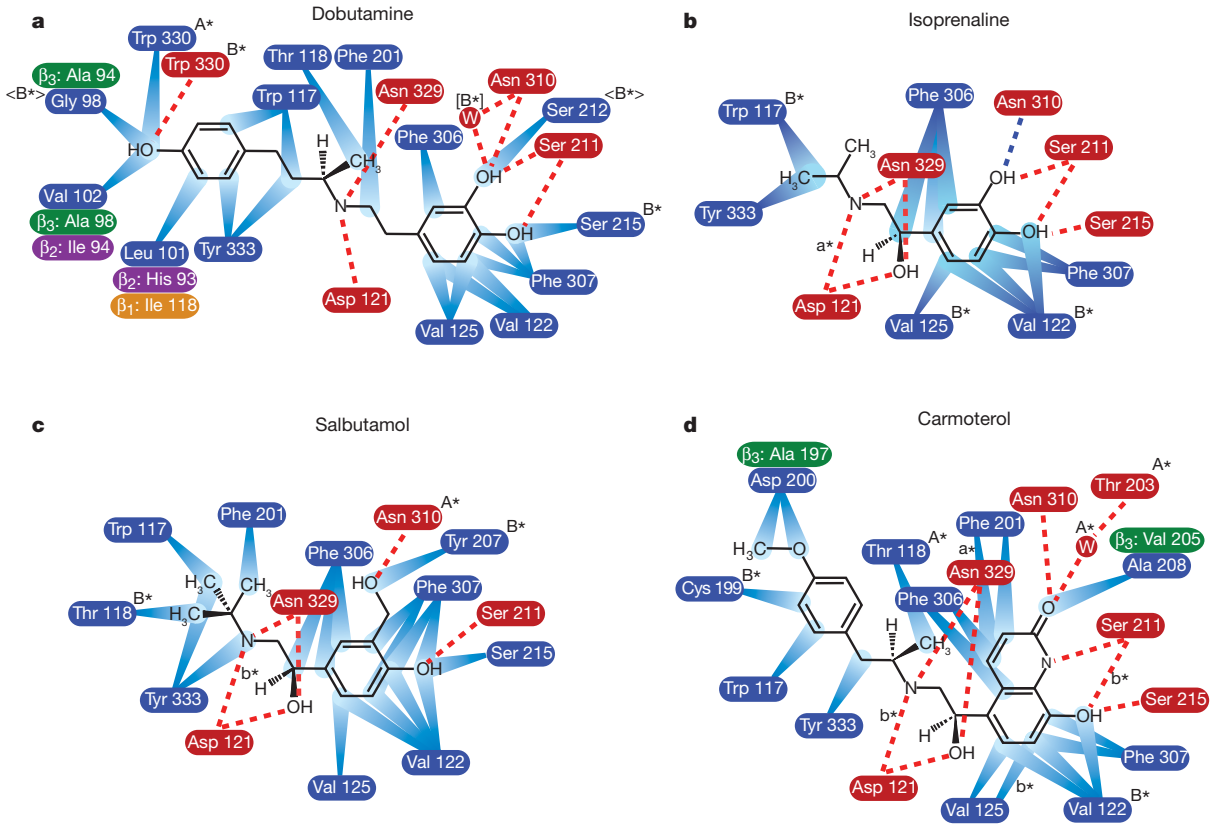

Figure 2 | Polar and non-polar interactions involved in agonist binding to β_1-adrenergic receptor. **a**–**d**, Amino acid residues within 3.9 Å of the ligands are depicted, with residues highlighted in blue making van der Waals contacts (blue rays) and residues highlighted in red making potential hydrogen bonds with favourable geometry (red dashed lines) or hydrogen bonds with unfavourable geometry (blue dashed lines). Amino acid residues labelled with an asterisk make the indicated contact either in monomer A (A*) or in monomer B (B*) only; for dobutamine, some contacts, labelled <B*>, are found only in monomer B of dob92, whereas another contact, labelled [B*], is found only in monomer B of dob102 (Supplementary Fig. 6 and also see Supplementary Table 6 for further details and for the Ballesteros–Weinstein numbering). If specific van der Waals interactions or polar interactions are found only in monomer A or B, then the interaction is labelled a* or b*, respectively. Where the amino acid residue differs between the turkey β_1AR and the human β_1AR, β_2AR and β_3AR, the equivalent residue is shown highlighted in orange, purple or green, respectively (see also Supplementary Table 7).

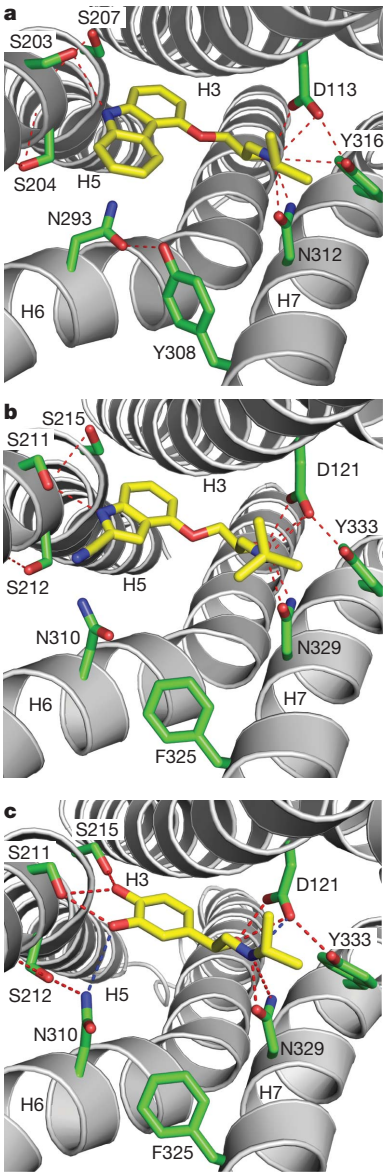

Figure 3 | Comparison of the ligand-binding pockets of the β_1 and β_2 adrenergic receptors. The ligand-binding pockets are shown as viewed from the extracellular surface with EL2 removed for clarity (same colour scheme as in Fig. 1). **a**, β_2AR with the antagonist carazolol bound (PDB code 2RH1); **b**, β_1AR with the antagonist cyanopindolol bound (PDB code 2VT4); **c**, β_1AR with the agonist isoprenaline bound.

between H4 and H5. As there is only a minimal interface between transmembrane helices H4 and H5 in this region (Supplementary Table 8 and Supplementary Fig. 8), this loss of interaction may be significant in the activation process. In this regard, it is noteworthy that the naturally occurring polymorphism in β_2AR at the H4–H5 interface, T164I$^{4.56}$, converts a polar residue to a hydrophobic residue as seen in β_1AR (Val 172$^{4.56}$), which results in both reduced basal activity and reduced agonist stimulation[21]. This supports the hypothesis that the extent of interaction between H4 and H5 could affect the probability of a receptor transition into the activated state.

In contrast to the apparent weakening of helix–helix interactions by the agonist-induced rotamer conformation change of Ser 215$^{5.46}$, the agonist-induced rotamer conformation change of Ser 212$^{5.43}$ probably results in the strengthening of interactions between H5 and H6. Upon agonist binding, Ser 212$^{5.43}$ forms a hydrogen bond with Asn 310$^{6.55}$ (Fig. 3) and, in addition, hydrogen bond interactions to Ser 211$^{5.43}$ and Asn 310$^{6.55}$ mediated by the ligand serve to bridge H5 and H6. The

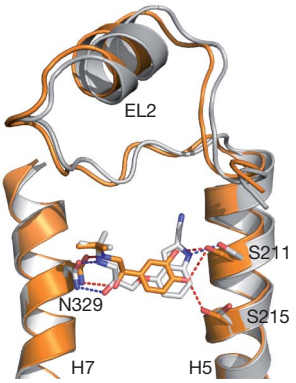

Figure 4 | Differences in the ligand-binding pocket between antagonist- and agonist-bound β_1-adrenergic receptor. An alignment was performed (see Methods) between the structures of β_1AR-m23 bound to either cyanopindolol (grey) or isoprenaline (orange) and the relative positions of the ligands and the transmembrane helices H5 and H7 are depicted. The 1 Å contraction of the ligand-binding pocket between H5 and H7 is clear.

combined effects of strengthening the H5–H6 interface and weakening the H4–H5 interface could facilitate the subsequent movements of H5 and H6, as observed in the activation of rhodopsin.

Stabilization of the contracted catecholamine binding pocket is probably the most important role of bound agonists in the activation process (Fig. 4). This probably requires strong hydrogen bonding interactions between the catechol (or equivalent) moiety and both H5 and H6, and strong interactions between the secondary amine and β-hydroxyl groups in the agonist and the amino acid side chains in helices H3 and H7. Reduction in the strength of these interactions is likely to reduce the efficacy of a ligand[29]. Both salbutamol and dobutamine are partial agonists of β_1AR-m23 (Supplementary Table 3) and human β_1AR. In the case of salbutamol, there are only two predicted hydrogen bonds between the headgroup and H5/H6, compared to three–four potential hydrogen bonds for isoprenaline and carmoterol. Dobutamine lacks the β-hydroxyl group, which similarly reduces the number of potential hydrogen bonds to H3/H7 from three–four seen in the other agonists to only two. We propose that this weakening of agonist interactions with H5/H6 for salbutamol and H3/H7 for dobutamine is a major contributing factor in making these ligands partial agonists rather than full agonists.

The agonist-bound structures of β_1AR indicate there are three major determinants that dictate the efficacy of any ligand: ligand-induced rotamer conformational changes of (1) Ser 212$^{5.43}$ and (2) Ser 215$^{5.46}$ and (3) stabilization of the contracted ligand-binding pocket. The full agonists studied here achieve all three. The partial agonists studied here do not alter the conformation of Ser 215$^{5.46}$ and may be less successful than isoprenaline or carmoterol at stabilizing the contracted catecholamine binding pocket due to reduced numbers of hydrogen bonds between the ligand and the receptor. The antagonist cyanopindolol acts as a very weak partial agonist and none of the three agonist-induced changes are observed. In contrast to partial agonists, neutral antagonists or very weak partial agonists such as cyanopindolol may also have a reduced ability to contract the binding pocket owing to the greater distance between the secondary amine and the catechol moiety (or equivalent). For example, the number of atoms in the linker between the secondary amine and the headgroup of cyanopindolol is four, whereas the agonists in this study only contain two (Fig. 1 and Supplementary Fig. 4). A ligand with a sufficiently bulky headgroup that binds with high affinity and which actively prevents any spontaneous contraction of the binding pocket and/or Ser$^{5.46}$ rotamer change, would be predicted to act as a full inverse agonist. This is indeed what is observed in the recently determined structure[15] of β_2AR bound to the inverse agonist ICI 118,551.

The significant structural similarities amongst GPCRs suggests that similar agonist-induced conformational changes to those we have

observed here may also be applicable to many other members of the GPCR superfamily, though undoubtedly there will be many subtle variations on this theme.

METHODS SUMMARY

Expression, purification and crystallization. The β44-m23 construct was expressed in insect cells, purified in the detergent Hega-10 and crystallized in the presence of cholesterol hemisuccinate (CHS), following previously established protocols[30]. Crystals were grown by vapour diffusion, with the conditions shown in Supplementary Table 4.

Data collection, structure solution and refinement. Diffraction data were collected from a single cryo-cooled crystal (100 K) of each complex in multiple wedges at beamline ID23-2 at ESRF, Grenoble, France. The structures were solved by molecular replacement using the β_1AR structure[13] (PDB code 2VT4) as a model (see Methods). Data collection and refinement statistics are presented in Supplementary Table 5.

Full Methods and any associated references are available in the online version of the paper at www.nature.com/nature.

Received 23 July; accepted 9 December 2010.

1. Evans, B. A. *et al.* Ligand-directed signalling at β-adrenoceptors. *Br. J. Pharmacol.* **159,** 1022–1038 (2010).
2. Rosenbaum, D. M., Rasmussen, S. G. & Kobilka, B. K. The structure and function of G-protein-coupled receptors. *Nature* **459,** 356–363 (2009).
3. Ballesteros, J. A. & Weinstein, H. Integrated methods for the construction of three dimensional models and computational probing of structure function relations in G protein-coupled receptors. *Methods Neurosci.* **25,** 366–428 (1995).
4. Strader, C. D. *et al.* Conserved aspartic acid residues 79 and 113 of the β-adrenergic receptor have different roles in receptor function. *J. Biol. Chem.* **263,** 10267–10271 (1988).
5. Sato, T., Kobayashi, H., Nagao, T. & Kurose, H. Ser^{203} as well as Ser^{204} and Ser^{207} in fifth transmembrane domain of the human β_2-adrenoceptor contributes to agonist binding and receptor activation. *Br. J. Pharmacol.* **128,** 272–274 (1999).
6. Liapakis, G. *et al.* The forgotten serine. A critical role for Ser-$203^{5.42}$ in ligand binding to and activation of the β_2-adrenergic receptor. *J. Biol. Chem.* **275,** 37779–37788 (2000).
7. Strader, C. D. *et al.* Identification of two serine residues involved in agonist activation of the beta-adrenergic receptor. *J. Biol. Chem.* **264,** 13572–13578 (1989).
8. Wieland, K. *et al.* Involvement of Asn-293 in stereospecific agonist recognition and in activation of the beta 2-adrenergic receptor. *Proc. Natl Acad. Sci. USA* **93,** 9276–9281 (1996).
9. Suryanarayana, S. & Kobilka, B. K. Amino acid substitutions at position 312 in the seventh hydrophobic segment of the beta 2-adrenergic receptor modify ligand-binding specificity. *Mol. Pharmacol.* **44,** 111–114 (1993).
10. Kikkawa, H., Isogaya, M., Nagao, T. & Kurose, H. The role of the seventh transmembrane region in high affinity binding of a β_2-selective agonist TA-2005. *Mol. Pharmacol.* **53,** 128–134 (1998).
11. Isogaya, M. *et al.* Identification of a key amino acid of the β_2-adrenergic receptor for high affinity binding of salmeterol. *Mol. Pharmacol.* **54,** 616–622 (1998).
12. Cherezov, V. *et al.* High-resolution crystal structure of an engineered human β_2-adrenergic G protein-coupled receptor. *Science* **318,** 1258–1265 (2007).
13. Warne, T. *et al.* Structure of a β_1-adrenergic G-protein-coupled receptor. *Nature* **454,** 486–491 (2008).
14. Hanson, M. A. *et al.* A specific cholesterol binding site is established by the 2.8 Å structure of the human β_2-adrenergic receptor. *Structure* **16,** 897–905 (2008).
15. Wacker, D. *et al.* Conserved binding mode of human β_2 adrenergic receptor inverse agonists and antagonist revealed by X-ray crystallography. *J. Am. Chem. Soc.* **132,** 11443–11445 (2010).
16. Tate, C. G. & Schertler, G. F. Engineering G protein-coupled receptors to facilitate their structure determination. *Curr. Opin. Struct. Biol.* **19,** 386–395 (2009).
17. Kobilka, B. K. & Deupi, X. Conformational complexity of G-protein-coupled receptors. *Trends Pharmacol. Sci.* **28,** 397–406 (2007).
18. Park, J. H. *et al.* Crystal structure of the ligand-free G-protein-coupled receptor opsin. *Nature* **454,** 183–187 (2008).
19. Scheerer, P. *et al.* Crystal structure of opsin in its G-protein-interacting conformation. *Nature* **455,** 497–502 (2008).
20. Engelhardt, S., Grimmer, Y., Fan, G. H. & Lohse, M. J. Constitutive activity of the human β_1-adrenergic receptor in β_1-receptor transgenic mice. *Mol. Pharmacol.* **60,** 712–717 (2001).
21. Green, S. A., Rathz, D. A., Schuster, A. J. & Liggett, S. B. The Ile164 β_2-adrenoceptor polymorphism alters salmeterol exosite binding and conventional agonist coupling to G_s. *Eur. J. Pharmacol.* **411,** 141–147 (2001).
22. Piscione, F. *et al.* Effects of Ile164 polymorphism of beta$_2$-adrenergic receptor gene on coronary artery disease. *J. Am. Coll. Cardiol.* **52,** 1381–1388 (2008).
23. Serrano-Vega, M. J. & Tate, C. G. Transferability of thermostabilizing mutations between β-adrenergic receptors. *Mol. Membr. Biol.* **26,** 385–396 (2009).
24. Serrano-Vega, M. J., Magnani, F., Shibata, Y. & Tate, C. G. Conformational thermostabilization of the β1-adrenergic receptor in a detergent-resistant form. *Proc. Natl Acad. Sci. USA* **105,** 877–882 (2008).
25. Balaraman, G. S., Bhattacharya, S. & Nagarajan, V. Structural insights into conformational stability of wild-type and mutant β_1-adrenergic receptor. *Biophys. J.* **99,** 568–577 (2010).
26. Altenbach, C. *et al.* High-resolution distance mapping in rhodopsin reveals the pattern of helix movement due to activation. *Proc. Natl Acad. Sci. USA* **105,** 7439–7444 (2008).
27. Rasmussen, S. G. *et al.* Crystal structure of the human β_2 adrenergic G-protein-coupled receptor. *Nature* **450,** 383–387 (2007).
28. Williams, R. S. & Bishop, T. Selectivity of dobutamine for adrenergic receptor subtypes: *in vitro* analysis by radioligand binding. *J. Clin. Invest.* **67,** 1703–1711 (1981).
29. Katritch, V. *et al.* Analysis of full and partial agonists binding to β_2-adrenergic receptor suggests a role of transmembrane helix V in agonist-specific conformational changes. *J. Mol. Recognit.* **22,** 307–318 (2009).
30. Warne, T., Serrano-Vega, M. J., Tate, C. G. & Schertler, G. F. Development and crystallization of a minimal thermostabilised G protein-coupled receptor. *Protein Expr. Purif.* **65,** 204–213 (2009).

Supplementary Information is linked to the online version of the paper at www.nature.com/nature.

Acknowledgements. This work was supported by core funding from the MRC and the BBSRC grant (BB/G003653/1). Financial support for G.F.X.S was also from a Human Frontier Science Project (HFSP) programme grant (RG/0052), a European Commission FP6 specific targeted research project (LSH-2003-1.1.0-1) and an ESRF long-term proposal. J.G.B. was funded by a Wellcome Trust Clinician Scientist Fellowship. We are grateful to P. Coli and A. Rizzi for the supply of (R,R)-carmoterol. F. Gorrec is thanked for his help with crystallisation robotics. We would also like to thank beamline staff at the European Synchrotron Radiation Facility, particularly D. Flot and A. Popov at ID23-2 and F. Marshall, M. Weir, M. Congreve and R. Henderson for comments on the manuscript.

Author Contributions T.W. devised and performed receptor expression, purification, crystallization, cryo-cooling of the crystals, data collection and initial data processing. P.C.E. helped with crystal cryo-cooling and data collection. J.G.B. performed the pharmacological analyses on receptor mutants in whole cells and R.N. performed the ligand binding studies on baculovirus-expressed receptors. R.M. and A.G.W.L. were involved in data processing and structure refinement. Manuscript preparation was performed by T.W., C.G.T., A.G.W.L. and G.F.X.S. The overall project management was by G.F.X.S. and C.G.T.

Author Information Coordinates and structure factors have been submitted to the PDB database under accession codes 2y00, 2y01, 2y02, 2y03 and 2y04 for β44-m23 bound either to dobutamine (dob92 and dob102), carmoterol, isoprenaline or salbutamol, respectively. Reprints and permissions information is available at www.nature.com/reprints. The authors declare no competing financial interests. Readers are welcome to comment on the online version of this article at www.nature.com/nature. Correspondence and requests for materials should be addressed to C.G.T. (cgt@mrc-lmb.cam.ac.uk) or G.F.X.S. (gebhard.schertler@psi.ch).

METHODS

Expression, purification and crystallization. The turkey (*M. gallopavo*) β_1AR construct, β36-m23, contains six thermostabilizing point mutations and truncations at the N terminus, inner loop 3 and C terminus[30]. Here we used the β44-m23 construct, which differs from the previously published β36-m23 construct only by the presence of two previously deleted amino acid residues at the cytoplasmic end of helix 6 (H6), Thr 277 and Ser 278. Baculovirus expression and purification were all performed as described previously[30], but with the detergent exchanged to Hega-10 (0.35%) on the alprenolol affinity column. Purified receptor was competitively eluted from the alprenolol Sepharose column with 0.2 mM agonist ((R)-isoprenaline, (R,S)-salbutamol, (R,S)-dobutamine or (R,R)-carmoterol). The buffer was exchanged to 10 mM Tris-HCl, pH 7.7, 100 mM NaCl, 0.1 mM EDTA, 0.35% Hega-10 and 1.0 mM agonist during concentration to 15–20 mg ml^{-1}. Before crystallization, CHS and Hega-10 were added to 0.45–1.8 mg ml^{-1} and 0.5–0.65%, respectively. Crystals were grown at 4 °C in 200 nl sitting drops and cryo-protected by soaking in either PEG 400 or PEG 600 for ~5 min (Supplementary Table 4) before mounting on Hampton CrystalCap HT loops and cryo-cooling in liquid nitrogen.

Data collection, structure solution and refinement. Diffraction data were collected at the European Synchrotron Radiation Facility, Grenoble, France, with a Mar 225 CCD detector on the microfocus beamline ID23-2 (wavelength, 0.8726 Å) using a 10-μm focused beam. The microfocus beam was essential for the location of the best diffracting parts of single crystals, as well as allowing several wedges to be collected from different positions. Images were processed with MOSFLM[31] and SCALA[32]. The isoprenaline complex was solved by molecular replacement with PHASER[33] using the β_1AR structure (PDB code 2VT4) as a model[13]. This structure was then used as a starting model for the structure solution of the carmoterol complex. Finally, the carmoterol complex was used as a starting model for both the dobutamine complexes and for the salbutamol complex. Refinement and rebuilding were carried out with REFMAC5[34] and COOT[35] respectively. The dob92 dobutamine crystal diffracted to a higher resolution (2.5 Å) than the dob102 crystal (2.6 Å), but the dob102 data set was more complete and less anisotropic than dob92 and gave a lower Wilson *B* factor (Supplementary Table 5). Dictionary entries for the agonists were created using Jligand and PRODRG[36]. During refinement with REFMAC5 tight non-crystallographic restraints ($\sigma = 0.05$ Å) were applied to the majority (172) of the residues in the two molecules in the asymmetric unit, with their selection based on improvements in R_{free} values. For the salbutamol complex, where the resolution was lower (3.05 Å), all three standard rotamers were modelled for Ser 211 and Ser 215 side chains, and the final choice was made on the basis of the local stereochemistry and features in the difference maps. Hydrogen bond assignments for the ligands were determined using hbplus[37] but allowing a maximum hydrogen-acceptor distance of 2.7 Å and a minimum angle of 89 degrees. Superposition of the different complexes was achieved by determining an initial transformation based on the 12 C-terminal residues of helix 2 (90–101) and then using the lsq_imp option of the program O[38] to find the largest number of residues that could be superposed without a significant increase in the root mean squared deviation (r.m.s.d.). Cutoff values of between 0.2–0.5 Å for residues to be included in the superposition were found to produce the largest number of residues while maintaining a small r.m.s.d. (<0.15–0.3 Å), depending on the structures being compared. This was repeated using the uppermost residues of helices 3, 6 and 7 to determine the initial transformation, and all cases converged to give the same solution, with 147 residues superposed and a final r.m.s.d. of 0.28 Å for the superposition of the carmoterol and cyanopindolol structures, and lower r.m.s.d. values for superposing different agonist structures on one another. The convergence to a common solution validates this procedure for determining the optimal transformation. Validation of the final refined models was carried out using Molprobity[39]. Omit densities for the ligands and the surrounding side chains are shown in Supplementary Fig. 3.

The two dobutamine crystals (dob92 and dob102) differed in the crystallization buffer and pH (Supplementary Table 4) and this resulted in slightly different unit cell parameters (Supplementary Table 5) and packing arrangements. The differences between these two structures (overall r.m.s.d 0.21 Å for monomer A, 0.21 Å for monomer B) provides a measure of the influence of crystal packing forces on the detailed conformation of the receptors. The observed differences in the ligand-binding pocket for monomer B, where there are no direct lattice contacts, emphasizes the conformational flexibility of this region (Supplementary Fig. 6).

Pharmacological analysis of agonist binding to the thermostabilized β_1AR mutants in whole cells. Stable CHO-K1 cell lines expressing either the wild-type turkey truncated receptor (βtrunc), or the β36, or the β6-m23 or the β36-m23 receptors and a CRE-SPAP reporter were used[40]. See Supplementary Table 1 for a description of the constructs. Cells were grown in Dulbecco's modified Eagle's medium nutrient mix F12 (DMEM/F12) containing 10% fetal calf serum and 2 mM D-glutamine in a 37 °C humidified 5% CO_2: 95% air atmosphere.

To analyse the affinities of agonist binding to β_1AR mutants ^{3}H-CGP 12177 saturation binding and competition binding experiments were performed on whole cells (Supplementary Table 1). Cell lines were grown to confluence in white-sided tissue culture 96-well view plates. ^{3}H-CGP 12177 whole-cell competition binding was performed as previously described[40] using ^{3}H-CGP 12177 in the range of 0.82–1.80 nM. The K_D values for ^{3}H-CGP 12177 were 0.32 nM (βtrunc), 0.85 nM (β6-m23), 0.34 nM (β36) and 0.88 nM (β36-m23). For the competition assays, all data points on each binding curve were performed in triplicate and each 96-well plate also contained six determinations of total and non-specific binding. In all cases, the competing ligand completely inhibited the specific binding of ^{3}H-CGP 12177. A one-site sigmoidal response curve was then fitted to the data using GraphPad Prism 2.01 and the IC_{50} was then determined as the concentration required to inhibit 50% of the specific binding as described previously[40].

The ability of the receptors to couple to G proteins and induce an increase in cAMP concentrations was determined by measuring the increase in secreted alkaline phosphatase (SPAP) under the transcriptional control of a cAMP response element (CRE). Cells were grown to confluence in clear plastic tissue culture treated 96-well plates and CRE-SPAP secretion into the media measured between 5 and 6 h after the addition of agonist as described previously (Supplementary Fig. 1 and Supplementary Table 3)[40].

Binding of agonists to β_1AR mutants expressed in insect cells for structural studies. Receptors β36 and β36-m23 were expressed using the baculovirus expression system in insect cells (High Five) as described previously[30]. Cells were disrupted by freeze-thaw and membranes prepared by centrifugation. Saturation binding and competition binding experiments were performed using ^{3}H-dihydroalprenolol as described previously[41]. Non-specific binding of radioligand to the receptor was determined by including 100 μM unlabelled alprenolol. The assay mixtures were incubated for 2 h at 30 °C and then filtered on a 96-well glass-fibre filter plates (Millipore) pre-treated with polyethyleneimine. The filters were washed three times with ice-cold buffer (Tris 20 mM pH 8, NaCl 150 mM), dried, and counted in a Beckmann LS 6000 scintillation counter. The apparent IC_{50} values were determined by nonlinear regression analysis using a one-site competition model in Prism software and K_i values were determined using the Cheng–Prusoff equation[42].

31. Leslie, A. G. W. The integration of macromolecular diffraction data. *Acta Crystallogr. D* **62,** 48–57 (2006).
32. Evans, P. Scaling and assessment of data quality. *Acta Crystallogr. D* **62,** 72–82 (2006).
33. McCoy, A. J. *et al. Phaser* crystallographic software. *J. Appl. Cryst.* **40,** 658–674 (2007).
34. Murshudov, G. N., Vagin, A. A. & Dodson, E. J. Refinement of macromolecular structures by the maximum-likelihood method. *Acta Crystallogr. D* **53,** 240–255 (1997).
35. Emsley, P., Lohkamp, B., Scott, W. G. & Cowtan, K. Features and development of *Coot*. *Acta Crystallogr. D* **66,** 486–501 (2010).
36. Schüttelkopf, A. W. & van Aalten, D. M. *PRODRG*: a tool for high-throughput crystallography of protein-ligand complexes. *Acta Crystallogr. D* **60,** 1355–1363 (2004).
37. McDonald, I. K. & Thornton, J. M. Satisfying hydrogen bonding potential in proteins. *J. Mol. Biol.* **238,** 777–793 (1994).
38. Jones, T. A., Zou, J. Y., Cowan, S. W. & Kjeldgaard, M. Improved methods for building protein models in electron-density maps and the location of errors in these models. *Acta Crystallogr. A* **47,** 110–119 (1991).
39. Davis, I. W. *et al.* MolProbity: all-atom contacts and structure validation for proteins and nucleic acids. *Nucleic Acids Res.* **35,** W375–W383 (2007).
40. Baker, J. G., Hall, I. P. & Hill, S. J. Agonist actions of "β-blockers" provide evidence for two agonist activation sites or conformations of the human β_1-adrenoceptor. *Mol. Pharmacol.* **63,** 1312–1321 (2003).
41. Warne, T., Chirnside, J. & Schertler, G. F. Expression and purification of truncated, non-glycosylated turkey beta-adrenergic receptors for crystallization. *Biochim. Biophys. Acta* **1610,** 133–140 (2003).
42. Cheng, Y.-C. & Prusoff, W. H. Relationship between the inhibition constant (K_i) and the concentration of inhibitor which causes 50 per cent inhibition (I_{50}) of an enzymatic reaction. *Biochem. Pharmacol.* **22,** 3099–3108 (1973).